Optical nanoscopy characterization of nanofilms

P C Montgomery[1*], P Chapuis[2,3], A Leong-Hoï[1], F Anstotz[1], A Rubin[2], J Baschnagel[2], C Gauthier[2], G Reiter[3] and G B McKenna[4]

[1] Laboratoire des Sciences de l'Ingénieur, de l'Informatique et de l'Imagerie (ICube), Unistra-CNRS, 23 rue du Loess, 67037 Strasbourg, France.
[2] Institut Charles Sadron (ICS), 23 rue du Loess, Strasbourg, France.
[3] Institute of Physics, University of Freiburg, Hermann-Herder-Str. 3, 79104 Freiburg Germany.
[4] Texas Tech University, Dept. of Chemical Eng., Box 43121, Lubbock, TX 79409−3121, USA.

E-mail: paul.montgomery@unistra.fr

Abstract. Glass formation and glassy behavior remains an important field of study in condensed matter physics, with many aspects still little understood. The approach used in this work is to observe the changes in behavior of glass-forming materials at the nanometer scale by exploring the viscoelastic properties of ultrathin free-standing glassy polymer films. An experimental measurement cell based on the nanobubble inflation method is used, consisting of inflating a polymer film suspended over an array of 5 µm diameter holes in a Si wafer. Measuring the deformation as a function of time as the material relaxes is used to determine the creep compliance. Both polystyrene (PS) and poly(vinyl acetate) (PVAc) films of a few tens of nm thickness prepared by spin-coating from solution have been studied. Interference microscopy is used to measure the deformation over several hours, which is challenging at the nanoscale due to mechanical deformations and drift. In this paper we present some of the first solutions developed to allow consistent measurements of film deformation using this novel interference nanoscopy technique. Future work will involve the measurements of creep compliance as a function of different film properties so as to be able to compare the results with theoretical predictions.

1. Introduction

Glass formation and glassy behavior remains an important field of study in condensed matter physics, with many aspects still little understood. An important parameter to consider is the glass transition temperature, T_g, below which glassy materials remain in the glassy state. Above T_g, the materials are in the molten or rubber-like state. It is this property that has allowed significant increases in fuel saving, for example in the aeronautic and automotive industries, through the use of lighter polymer composites to replace metal parts. In bulk materials, T_g remains constant, an important factor for structural design criteria and safe performance. On the contrary, when one of the dimensions is less than about 1 µm, for example in thin films, T_g decreases with thickness [1], which could be problematic for certain industrial applications. One approach to this problem is therefore to observe the changes in behavior of glass-forming materials at the nanometer scale. Some studies state that confinement and/or interfacial physics lead to different behavior for ultra-thin free-stranding polymer films [1, 4]. For example, preparing the film by spin-coating results in an out-of-equilibrium state of

the polymer chains [2]. In this work, the viscoelastic properties of ultrathin free-standing glassy polymer films are explored according to the preparation process employed, using an experimental measurement cell based on the nanobubble inflation method [3]. This technique consists of inflating a polymer film suspended over an array of 5 μm diameter holes in a Si wafer held in the cell. Measuring the deformation as a function of time as the material relaxes is used to determine the creep compliance. Using this arrangement, there is no substrate interaction to affect the polymer chains. This is the first part of a longer term project to study the properties of different types of films having a thickness of several tens of nm prepared by different means in order to obtain a deeper insight into the viscoelastic behavior of such ultrathin glassy films.

Both PS and PVAc films of a few tens of nm thickness have been prepared by spin-coating from solution in toluene onto a Si wafer and manually transferring the film onto the perforated substrate using a water bath. Interference microscopy is used to measure the change in deformation over several hours. This technique is one of a family of new unlabeled nanoscopy techniques, consisting of far field optical microscopy that is used for extracting useful structural and physical information from nanostructures [5]. Coherence scanning interferometry (CSI) or white light scanning interferometry (WLSI) as it is also known, using polychromatic illumination, is more commonly used for the measurement of surface roughness and 3D microscopic surface structure [6]. We have adapted this technique to many different applications including the measurement of microelectronic components [7], microsystems [8], biomaterials [9] and colloids [10]. Phase shifting microscopy (PSM), which uses monochromatic or quasi-monochromatic illumination, is used for the measurement of small roughness and surface structures, for example on the surface of optical components [11] and semiconductor materials [12].

Compared with AFM, while interference microscopy is limited in lateral resolution to about $\lambda/2$ (typically about 0.4 μm), it has the advantages of being non-contacting, having a much wider field of view and with a much faster acquisition time. For example, a typical measurement of a static surface using PSM takes only several seconds [13] compared with a typical time of up to 10 minutes or more with AFM. For measurements of periodically moving surfaces, strobing can be used to freeze the surface and PSM used to measure deformations for example in micromirrors up to frequencies of several MHz [14]. In the case of aperiodic motion, real time measurement of changing surfaces has been achieved using a high speed camera and FPGA processing [15]. Although the axial sensitivity of interference microscopy can be better than 1 nm, achieving high accuracy at the nanoscale can be a challenge [16]. Nanoscale measurements of a surface deforming over several hours presents further difficulties due to mechanical deformations and drift. In this paper we present some of the first solutions that we have developed to allow the consistent measurements of film deformation using this novel interference nanoscopy technique.

2. Nano-bubble inflation method

In this section the nanobubble inflation method is explained, showing how measurement of the deformation of nanobubbles over time can be used to determine the creep compliance of the material.

2.1. Experimental measurements of deformation

The polymer film is placed over an array of holes 5 μm in diameter. Measured with AFM, the freestanding film is deformed downwards into the hole by capillary forces (figure 1(a)) [17]. When the array of holes is placed on a pressure cell fed with a supply of air or nitrogen gas in order to inflate the nanobubbles to a set pressure, the nanobubbles inflate. While this deformation can be measured with AFM (figure 1(b)), the technique is not practical for measurements over periods of several hours. The aim of the present work is to use interference microscopy to measure the surface contour of the nanobubble and thus the radius of curvature. If the nanobubble is inflated at room temperature, the deformation is very small even over a period of several hours. The sample needs to be heated up and maintained at constant temperature close to T_g, for example using a Peltier cell. For bulk polymers, T_g

is constant and according to the literature, the values of T_g for nanofilms is less than that for the bulk material [18].

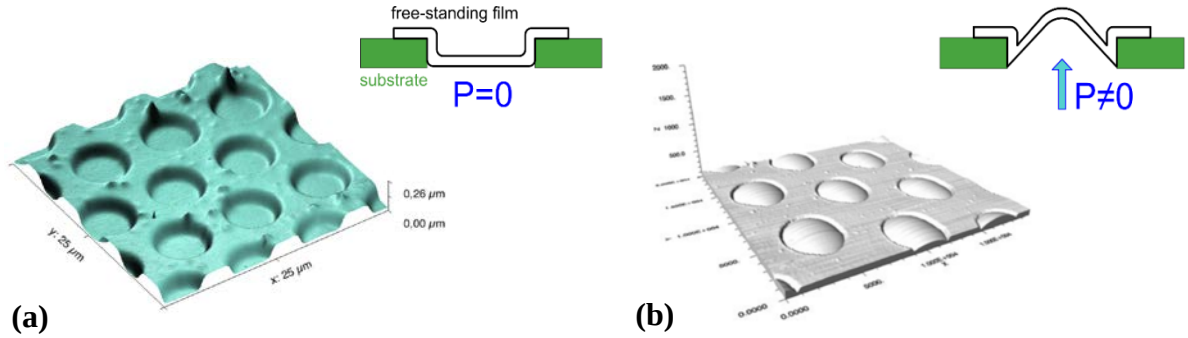

Figure 1. Examples of AFM measurements of films on 5 µm hole grid substrates (a) 90 nm thick PS film with T = RT and P = 0 Pa. Deflection due to capillary forces during the annealing process and (b) inflated 17 nm thick PS film with T = 57 °C and P = 1 psi (≈ 69 kPa) [17].

2.2.Method for estimation of creep compliance

The method used to estimate the creep compliance *D(t)* is the Boltzmann superposition principle for a spherical sample by taking into account the history of the polymer. The first step is to measure the surface contour of the nanobubble at regular intervals over the time period of the experiment (several hours). Then for a contour at a given time, the curvature κ and the radius of curvature *R* are estimated for the average line profile passing through the centre of the circle of the nanobubble by fitting this profile with a second order polynomial *y* and by using the following equations:

$$\kappa = \frac{|y''|}{(1+y'^2)^{3/2}} \qquad R = 1/\kappa$$

This calculation is performed for all the contour measurements of the nanobubble. Then the biaxial components of the stress, σ and the strain, ε are estimated from the radius as a function of time [3]:

$$\sigma = \frac{PR}{2t} \qquad \epsilon = \frac{2Rsin^{-1}\left(\frac{R_0}{R}\right)}{2R_0} - 1$$

where *P*, *t*, R_0 and *R* are respectively the pressure, the film thickness, the hole radius and the radius of curvature. The Boltzmann superposition principle is then applied to obtain the creep compliance (here *t* denotes time):

$$\epsilon(t) = \int_0^t \sigma(t-\xi)\left[\frac{dD(\xi)}{d\xi}\right]d\xi + D_g\sigma(t)$$

where $\varepsilon(t)$, $\sigma(t)$, $D(t)$ and D_g are respectively the time dependent biaxial strain, the time dependent biaxial stress, time dependent biaxial creep compliance and the instantaneous glassy biaxial creep compliance. $D(t)$ is then obtained from all the values of $\Delta D(t)$ estimated from the fits of the experimental data ($\sigma = f(t)$ and $\varepsilon = f(t)$).

3. Experimental techniques

In this section, the details of the experimental techniques are given, concerning the preparation of the polymer film samples, the design of the pressure cell and the interference microscopy technique employed to make the deformation measurements.

3.1. Sample preparation

The PS films were prepared by first making a solution of ~1.5% PS/toluene (w/w), with Mw PS = 125 kDa and PDI PS = 1.05. For the PVAc films, these values were ~ 3.0 % PVAc/toluène (w/w), with Mw PVAc = 100 kDa and PDI PVAc = 1.05. To make a film, a clean Si wafer is covered by a thin film of PS or PVAc solution which is then spin-coated at a speed of 2000 rpm. The film is then transferred onto the perforated substrate by floating it in a clean water bath and the samples are allowed to dry overnight in air before finally annealing in an oven for 1 hr at a temperature of T_g + 10°C.

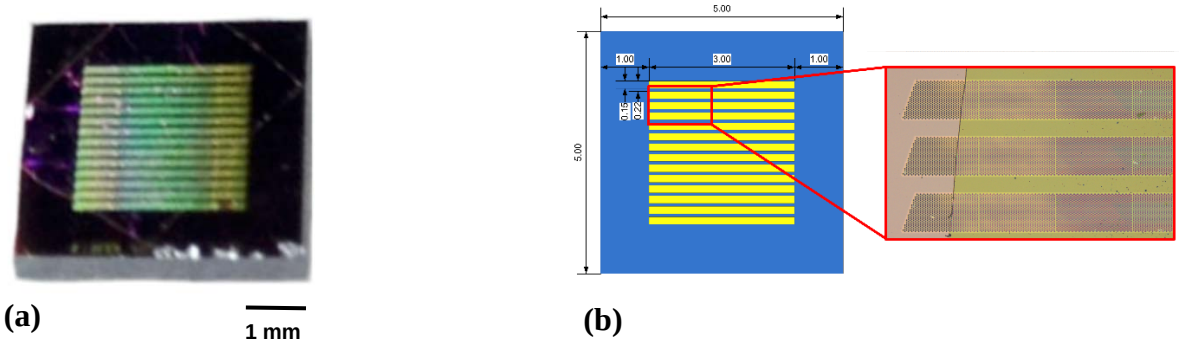

Figure 2. Details of the Si grid substrate (a) photo of Si grid and (b) design of Si substrate (left) and optical microscopy image of small region (right) showing 5 µm holes array with thin PS polymer film (area of greenish tinge); distances in mm.

The perforated grid used is a micro sieve type filter from Aquamarijn Micro Filtration BV (The Netherlands) made by a stencil lithography method [19]. The model employed consists of a very thin (0.9 µm) perforated Si_3N_4 membrane with closely spaced holes 5 µm in diameter in 14 bands (0.15 mm x 3 mm) on a 0.4 mm thick Si support (figure 2). After the deposition of the film, the samples are stored at 30°C ±3°C.

Visual inspection of the polymer film is first performed using optical reflection microscopy. Such an image of the film can be observed in figure 2(b) (far right), the area of greenish tint showing the position of the film placed over the grid of holes.

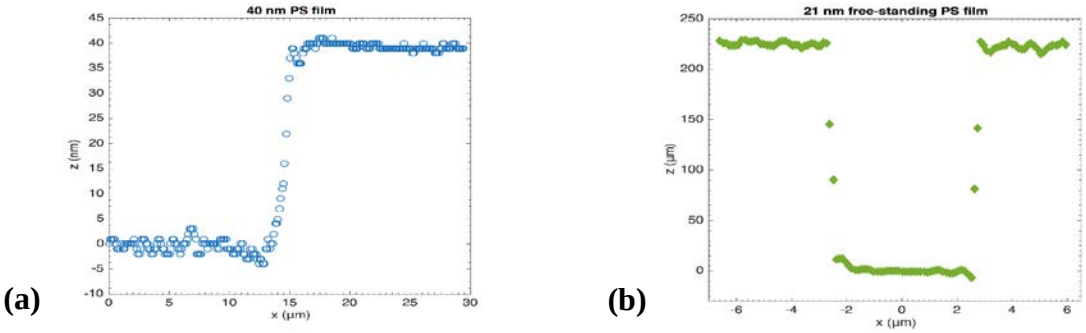

Figure 3. Measurements of PS polymer films using AFM: (a) 40 nm film thickness as measured at edge after placing on grid (b) deflection within hole of a 21 nm thick free standing film due to capillary forces during the annealing process.

Two types of measurements were performed with AFM on a JPK BioMAT Workstation model. First the film thickness was measured near to the edge of the film on a flat part of the perforated grid. An example showing a film thickness of 40 nm of one of the samples is shown in figure 3(a). Then,

the shape of a free standing film on one of the holes was measured, the results in figure 3(b) showing a deflection due to capillary forces of about 230 nm into the hole.

3.2. Pressure cell

The pressure cell was designed so as to be able to control the pressure and temperature of the film on the perforated grid (figure 4). The cell was made in aluminium so as to be light enough to be able to be placed on the piezo table (figure 5) for performing fringe scanning. The pressure was provided underneath the film through a hole in the cell by gas from a bottle of nitrogen delivered through a low pressure regulator valve. The pressure could thus be varied over a range of 0-400 kPa. The sample was placed in the middle of a Peltier ring (figure 4) in order to be able to control the temperature from room temperature to 80°C. The temperature of the sample was calibrated using a thermocouple temporarily stuck to the top of an older perforated grid.

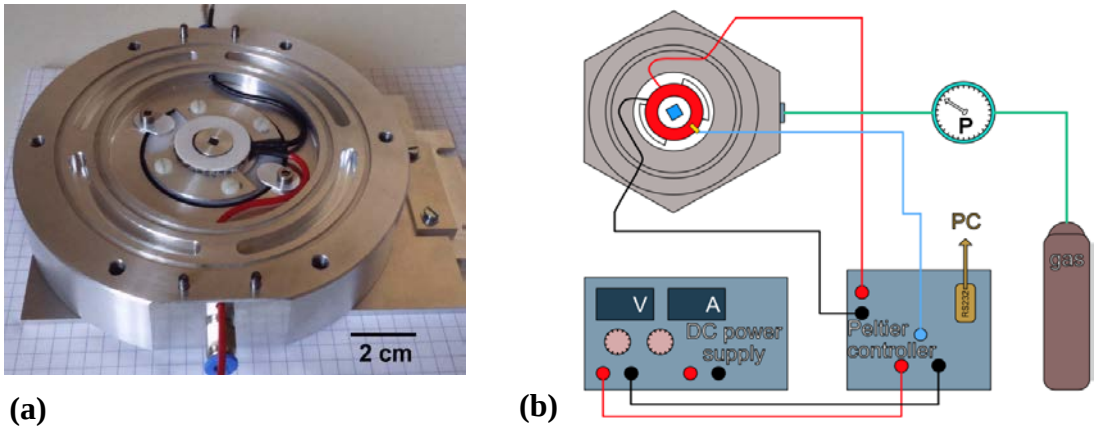

Figure 4. Details of the pressure cell (a) photo of pressure cell and (b) layout of pressure cell and control of pressure and temperature.

As stated previously, for performing the nanobubble experiments, the temperature of the film was raised to just close to the glass transition temperature of the bulk polymer ($T_g \approx 100$°C for PS).

3.3. Interference microscopy

The deformation measurements of the nanobubbles were made using a modified Leitz-Linnik interference microscope [20] with identical x50 (NA = 0.85) objectives and an incandescent light source. A Pifoc piezoelectric nanopositioner (from PI) controlled in a closed loop with a capacitive position sensor was used for the Z-scanning of the fringes over the depth of the sample (figure 5). Images are acquired with a color CCD camera (Basler avA1000-100gc) with a Giga Ethernet connection. The measurement system is controlled by a PC equipped with an Intel® Xeon® CPU processor (2.40 GHz, 8 Go RAM) under a Windows 7 (64 bits) operating system. The control and analysis software was developed in-house under LabVIEW (version 2014, 64 bits, from National Instruments) combined with the IMAQ Vision module.

The Linnik configuration of the interferometer (figure 5) has the advantages of being able to use high NA objectives, giving a better lateral resolution than the Mirau or Michelson type arrangements [21]. The Linnik interferometer is adjusted first to produce high contrast fringes superimposed on the surface of the film by modifying the path length difference between the two arms to match the coherence planes. The fringes are orientated parallel to the band of holes. The algorithm used to make the phase measurement was a modified version of the 5 phase step algorithm (five steps of $\pi/2$), together with image averaging of 5 frames, which is a good compromise between noise reduction and acquisition time and light (3x3 pixels) median/low pass filtering to reduce the camera noise [20]. Due

to the 2π phase discontinuities, the PSM algorithm only allows height measurements up to λ/2 (< 300 nm at λ = 600 nm). However, the nanobubble growth can achieve a height above 300 nm. This problem can be solved by synchronizing the algorithm with a careful shift control of the piezoelectric table. In this work, a single acquisition with averaging takes ~5 seconds and the whole measurement procedure ~2 minutes, due to manual adjustment of the setup and storing of the results.

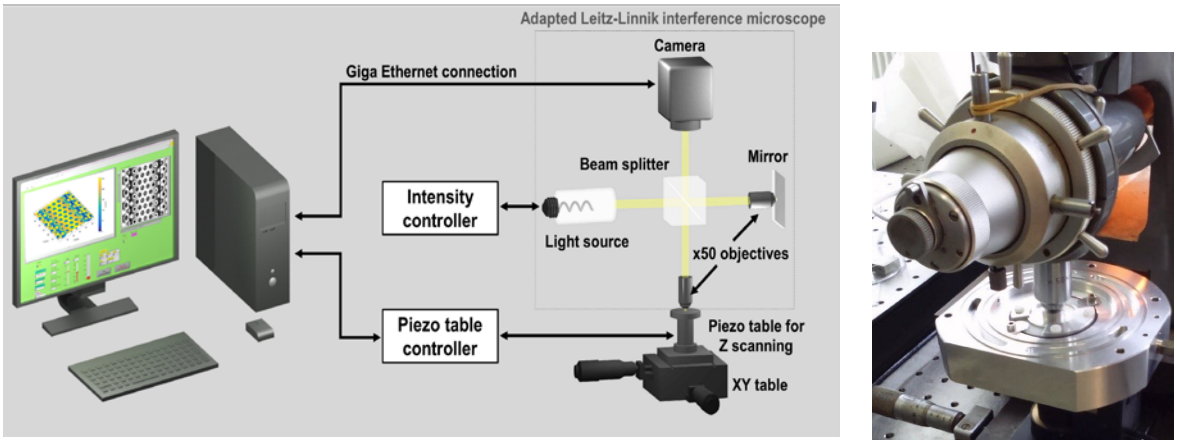

Figure 5. Details of the Leitz-Linnik interference microscope system used for nano-3D measurements (a) Schematic layout of system and (b) close-up of the Linnik interferometer and pressure cell.

4. Measurements of the viscoelastic response with time

Making a single measurement of the film surface shape at a given time is fairly straightforward. With a correct disposition of the fringes, the phase shifting technique results in a phase map that can then be converted to height to give a contour map with nm axial sensitivity. Some typical results of a single measurement of the freestanding film are given in figure 6, showing the measurements at two successive steps of post-processing to reduce the noise. The sudden jumps in phase across the image visible in figures 6(a) and (b) are due to the 2π phase discontinuities resulting from the phase shifting technique which results in an axial range limited to λ/2. In smoothly changing surfaces, the phase can be unwrapped [22] but in the presence of noise or sharp steps, phase unwrapping is not so easy. In these first measurements, due to the presence of noise, by means of a careful choice of the axial position and fringe orientation, direct measurements can be made and the profile read directly (figure 6(c)).

To measure the viscoelastic response of the film, the nanobubble has to be heated to the required stable temperature, inflated to a certain value of pressure and then left to deform over a period of up to several hours. Measurements of the surface contour are then made at regular intervals. The challenge in the present work is to make a series of surface contour measurements over this period of time that can be related to each other meaningfully. When making measurements at the nanoscale, deformations and drift result in profiles that do not seem to be related, since measurements are made on an absolute axial scale.

Several attempts were made to measure the deformation of the nanobubbles over time using the interference technique before arriving at a protocol that enabled fairly consistent results to be obtained of the local deformation. In the following section, some typical results of the measurements are given, together with a discussion of the challenges faced in measuring at the nanoscale and a presentation of some of the first calculations of the viscoelastic response over time.

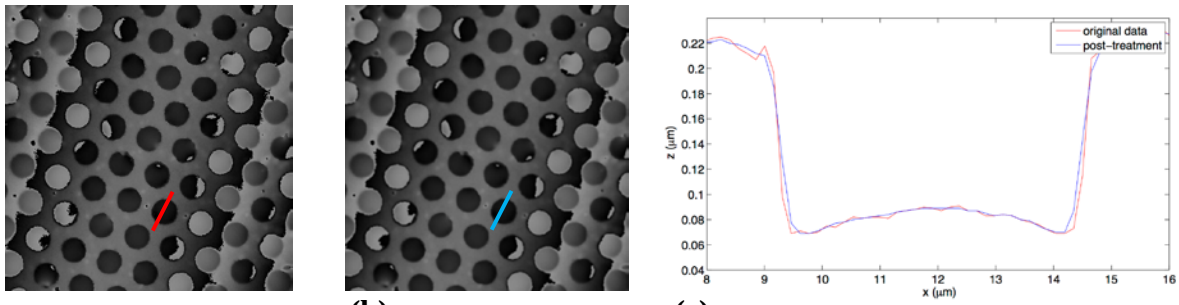

Figure 6. Some of the first results of measurements of the surface contour of a freestanding PS polymer film (50 µm x 50 µm region) (a) the phase measurement after median filtering, (b) the phase measurement after median filtering and low pass filtering and (c) profiles of the film over one of the holes after conversion of the phase to height, showing the original data (red line) and after post-processing (blue line).

4.1. Typical measurement results using interferometry

The results in figure 7 show some typical surface contours of an inflated film during one of the experiments measured with the protocol developed. The phase measurements can be observed in figure 7(a), in the presence of phase discontinuities and the associated height contours can be seen in figure 7(b). The correct positions of the nanobubbles is below the surface of the grid, as can be observed in the center near to the line x = 30 µm. To make these nanobubbles visible for the purposes of observation (inset in figure 7(b)), they are "virtually" raised above the level of the grid by using image processing on a small portion of the image to detect the positions of the holes and to apply a mask with an intensity of 0 to lower the surrounding grid.

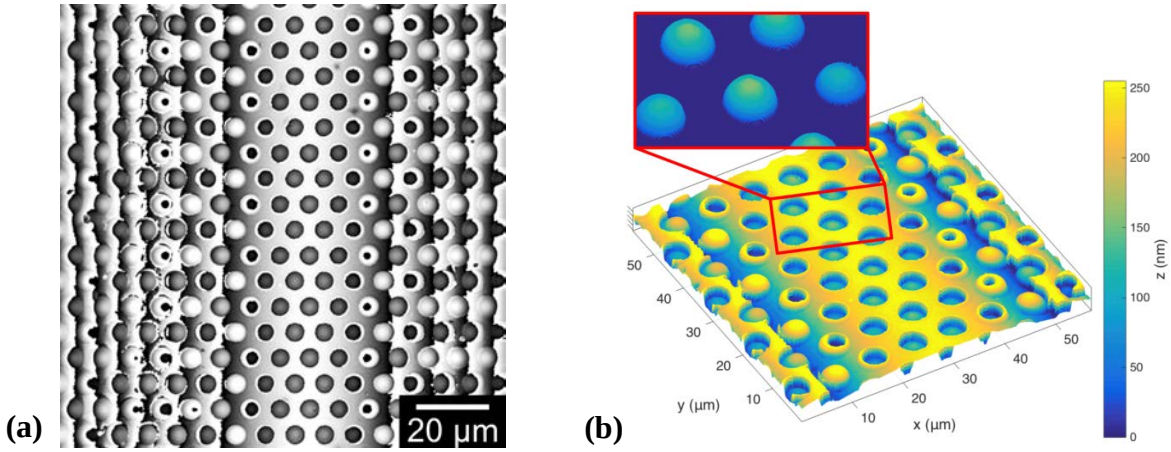

Figure 7. Some of the first results of measurements of the surface contour of an inflated PS polymer film during one of the experiments (a) a 2D image of the measured phase and (b) a 3D image of the height taken from the central region of (a); inset: bubble shapes visualization by hiding the grid.

4.2.Challenges faced in measuring deformation at the nanoscale

As previously noted, measuring the deformation of the nanobubbles at the nanoscale over a period of several hours is challenging. Several of the difficulties met with have already been overcome and some of the solutions developed are now described:

Choice of PSM algorithm for fringe interpretation – Considering that the substrate moves axially over a distance of several μm due to various deformations, a more appropriate fringe interpretation algorithm would have been an envelope detection algorithm in white light. This is commonly used in the measurement of deep surface roughness [21] but with the drawback of having a limited axial sensitivity of about 10-15 nm. Although this value can be improved by combining envelope detection with phase measurement [23, 24], errors at the nm scale can still appear in the case of the presence of steps as in the sample under study. Since the sample was unknown at the beginning of the study, it was therefore decided to use the phase shifting technique, combined with a shift control of the piezoelectric nanopositioner to follow the nanobubble growth, without phase unwrapping so as to stick more closely to the raw data and reduce the number of possible errors. The technique employed was therefore first to align the array of holes symmetrically with the camera field of view and then to optimize the contrast and orientation of the fringes in the Linnik interferometer.

Effects due to the change in temperature – Since some of the samples were heated up to 70°C, it was necessary to wait 1 hr to reach thermal equilibrium, both of the sample cell and the microscope. This was observable by movement of the fringes at the beginning of the heating cycle due to expansion of the different mechanical parts. This movement stabilized after 1 hr. Unknown aspects worth investigating would be the effect of the change in temperature on the sample objective and Linnik interferometer.

Effects due to the pressure – Once the temperature effects were stabilized, several effects on the measurements resulted from the application of the pressure on the film and pressure cell:

1. First, the overall deformation was found to be semi-cylindrical which can be observed in figure 7(a) by the symmetrically arranged phase discontinuities and in figure 7(b) by the curved aspect of the 3D measurement. This is due to the rectangular shape of the array of holes (3 mm x 150 μm) which results in cylindrical deformation under pressure. Taking a profile across the short width of the array of holes therefore gives a curved profile. To avoid the need for correction, the fringes were simply aligned parallel to the longer length of the grids so that the line profiles of the nanobubbles were nearly flat at the center (in the direction of the grid deformation (figure 7(a)).
2. A second effect of the pressure is vertical drift over time of the overall position of the sample along the optical axis, due to the deformation of the substrate and holder. This effect is corrected between measurements by refocusing. Finer adjustment of the fringe position is achieved by using the offset of the piezo nanopositioner, a function which is written into the controlling software.
3. A third effect of the pressure is fast nanobubble growth over the first 10 minutes. Since the present measurement procedure takes ~2 minutes, this means that data acquisition is limited over this important initial period of deformation.

Possible sources of measurement error – After this initial study of the technique for deformation measurement, several other possible sources of error are suggested:

1. Is there a phase on reflection error of the measured wavefront from the sample between the polymer film and the film on the silicon nitride hole array support? Since these materials are both dielectric, in principle this should not be the case, but there could still be some thin film effects. Simulation could help answer this question.
2. Are there edge artefacts of individual nanobubbles influencing the reconstruction of the surface profile of the film? This could be investigated by making different measurements at various tilt angles of the sample.
3. A comparison of the edge measurements of the nanobubble profiles shows the edge positions to be moving upwards (figure 8(a)). Is this due to slipping of the polymer film due to it unsticking at the edge or is it due to the measurement method, or both?

4.3. Interpretation of the deformation measurements

The results in figure 8(a) consist of a set of typical measurements, showing the change in the measured profile of a PVAc nanobubble as a function of time over a period of just over 3 hrs. They show a decreasing rate of inflation with time. Using the method described in section 2.2, the creep compliance was then calculated step by step as a function of time by taking into account the stress and strain histories, giving the plot in figure 8(b). What this curve shows is that after a given time, the polymer reaches the rubbery plateau. This means is that at this step, the polymer chains in the film are very entangled while the chain segments are very mobile. Because of this, the whole chain is impeded and the creep compliance becomes and remains constant in time.

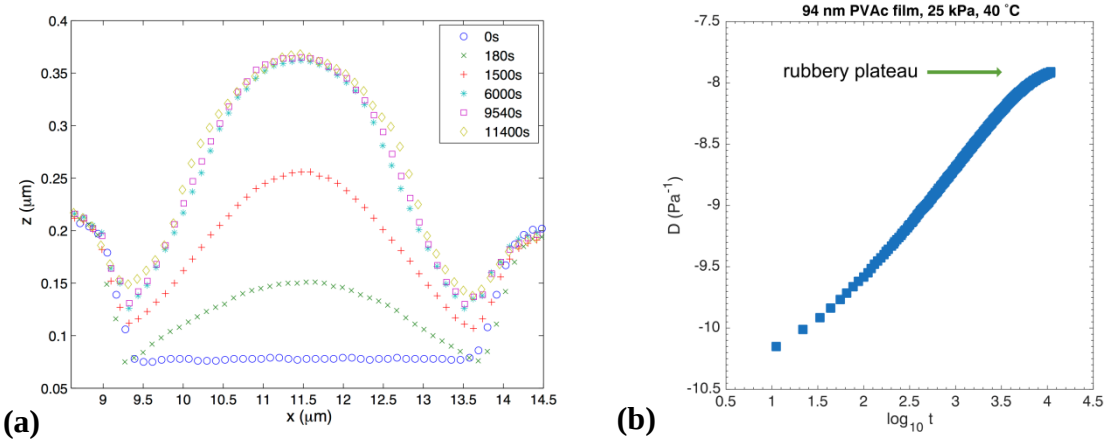

Figure 8. One set of results of measurements made on a PVAc film nanobubble (a) profiles of the nanobubble at different times and (b) plot of the creep compliance, $\log_{10} D(t)$ versus $\log_{10} t$ (in seconds), from the profile in (a), estimated using the described method.

5. Conclusions

The aim of this work was to investigate the glassy behavior of materials by studying the viscoelastic responses with time of freestanding polymer nanofilms using the Boltzmann superposition principle for spherical samples. The nanobubble inflation method was used in combination with interference microscopy for measuring the surface contour of the nanobubbles over time. To this end, an adapted pressure and temperature cell was specially developed for the microscope.

Measuring nanodeformation over a period of several hours is challenging, due to deformations and drift arising from the use of pressure and heating of the nanofilms. In this paper we have presented some of the first solutions developed to allow consistent measurements of film deformation using a novel interference nanoscopy technique.

Further work is necessary in order to reduce even further the noise and artefacts in the measurement of the surface contour of the nanobubble, such as by improving the optical quality of the Linnik interferometer and by using quasi-monochromatic illumination light. The measurement time could also be reduced well below 2 minutes by automating the acquisition, processing and adjustment procedure.

Future work will then involve the measurements of creep compliance as a function of different film properties, pressures, aging times and Mw. These results will be then compared with existing data measured by AFM [3, 17] with the aim of providing reference data for the viscoelastic behavior of polymer nanofilms, similarly to those existing in the bulk.

6. Acknowledgements
Thanks are given to Damien Flavier for developing the temperature controller, to Stéphane Roques for installing the nitrogen gas pressure system, to Silvia Siegenführ and Asad Jamal for the AFM recommendations and to Sivasurender Chandran for helping with the sample preparation method. Special thank are extended to the IRTG "Soft Matter Science" (GRK 1642/2) for financial support.

References

[1] Forrest J A and Dalnoki-Veress K 2000 *Advances in Colloid and Interface Science* **94** 167
[2] Chowdhury M, Freyberg P, Ziebert F, Yang A C M, Steiner U and Reiter G 2012 *Physical Review Letters* **109** 136102
[3] O'Connell P A and McKenna G B 2005 *Science* **307** 1760
[4] Baschnagel J and Varnik F 2005 *J. Phys.: Condens. Matter* **17** R851
[5] Montgomery P, Leong-Hoi A, Anstotz F, Mitev D, Pramatarova L and Haeberle O 2016 *J. Phys. Conf. Series* **682** 012010
[6] De Groot P 2015 *Advances in Optics and Photonics* **7** 1
[7] Montgomery P, Fillard J P, Castagné M and Montaner D 1992 *Semicond. Sci. and Technol* **7** A237
[8] Montgomery P C, Montaner D, Manzardo O, Flury M and Herzig H P 2004 *Thin Solid Films* **450** 79
[9] Pecheva E, Montgomery P, Montaner D and Pramatarova L 2007 *Langmuir* **23** 3912
[10] Halter E, Montgomery P C, Montaner D, Barillon R, Del Nero M, Galindo C and Georg S 2010 *Applied Surface Science* **256** 6144
[11] Perrot O, Guinvarc'h L, Benhaddou D, Montgomery P C, Rimet R, Boulard B and Jacoboni C 1995 *J. Non-Crys. Solids* **184** 257
[12] Benatmane A, Montgomery P C, Fogarassy E and Zahorsky D 2003 *Applied Surface Science* **208-209** 189
[13] Schmit J, Reed J, Novak E and Gimzewski J K J 2008 *Opt. A: Pure Appl. Opt.* **10** 064001 1
[14] Petitgrand S and Bosseboeuf A 2004 *Journal of Micromechanics and Microengineering* **14** 9
[15] Montgomery P C, Anstotz F, Johnson G and Kiefer R 2008 *Mat. Sci.: Mat. in Elec.* **19** Suppl. 1 194
[16] Montgomery P C, Guellil M, Pfeiffer P, Serio B and Pramatarova L 2014 *J. Phys. Conf. Series* **558** 012005 1
[17] O'Connell P A, Hutcheson S A and McKenna G B 2008 *Journal of Polymer Science: Part B: Polymer Physics* **46** 1952
[18] Dalnoki-Veress K, Forrest J A, Murray C, Gigault C and Dutcher J R 2001 *Physical Review E* **63** 031801
[19] https://www.aquamarijn.nl/showcases/nanostencils/
[20] Montgomery P C, Montaner D and Salzenstein F 2012 *Proc. SPIE* **8430** 843014
[21] De Groot P 2015 *Handbook of Optical Metrology: Principles and Applications* (CRC Press, Boca Raton)
[22] Ghiglia D C and Pritt M D 1998 *Two-Dimensional Phase Unwrapping, Theory, Algorithms, and Software* (John Wiley & Sons, New York)
[23] Harasaki A, Schmit J and Wyant J C 2000 *Applied Optics* **39** 2107
[24] Montgomery P C, Montaner D, Salzenstein F, Serio B and Pfeiffer P 2013 *Proc. SPIE* **8788** 87883G